Are aptamers really promising as receptors for analytical purposes? Insights into anti-lysozyme DNA aptamers through a multi-technique study

Are aptamers really promising as receptors for analytical purposes? Insights into anti-lysozyme DNA aptamers through a multi-technique study

Lorenzo Toma[a], Monica Mattarozzi[a,b,*], Luca Ronda[c,d], Valentina Marassi[e,f,g], Andrea Zattoni[e,f,g], Simone Fortunati[a,g], Marco Giannetto[a,b,g], Maria Careri[a,b,g]

[a] Department of Chemistry, Life Sciences and Environmental Sustainability, University of Parma, 43124, Parma, Italy

[b] Interdepartmental Center SITEIA.PARMA, University of Parma, 43124, Parma, Italy

[c] Department of Medicine and Surgery, University of Parma, 43124, Parma, Italy

[d] Institute of Biophysics, CNR, 56124 Pisa, Italy

[e] Department of Chemistry, University of Bologna, Via Selmi 2, 40126, Bologna, Italy

[f] byFlow srl, 40126, Bologna, Italy

[g] INBB, National Institute for Biostructures and Biosystems, 00136, Rome, Italy

KEYWORDS Aptamers, lysozyme, magnetic beads, aptamer affinity, selectivity

ABSTRACT: Aptamers are recognition elements increasingly used for the development of biosensing strategies, especially in the detection of proteins or small molecule targets. Lysozyme, which is recognized as an important biomarker for various diseases and a major allergenic protein found in egg white, is one of the main analytical targets of aptamer-based biosensors. However, since aptamer-based strategies can be prone to artifacts and data misinterpretation, rigorous strategies for multifaceted characterization of aptamer-target interaction are needed. In this work a multi-technique approach has been devised to get further insights into the binding performance of the DNA anti-lysozyme aptamers commonly used in literature. To study molecular interactions between lysozyme and different anti-lysozyme DNA aptamers, measurements based on a magneto-electrochemical apta-assay, circular dichroism spectroscopy, fluorescence spectroscopy and asymmetrical flow field-flow fractionation were performed. The reliability and versatility of the approach were proved by investigating a SELEX-selected RNA aptamer reported in the literature, which acts as positive control. The results confirmed that an interaction in the low micromolar range is present in the investigated binding buffers and the binding is not associated with a conformational change of either the protein or the DNA aptamer. The similar behaviour of the DNA anti-lysozyme aptamers compared to that of randomized sequences and polythymine, used as negative controls, showed non-sequence-specific interactions. This study demonstrates that severe testing of aptamers resulting from SELEX selection is the unique way to push these biorecognition elements towards reliable and reproducible results in the analytical field.

INTRODUCTION

A bioreceptor is a natural, synthetic or bioinspired molecule with high binding affinity and selectivity towards a specific target analyte in presence of other compounds in the sample matrix. Over the past 30 years, aptamers have attracted considerable attention not only for targeted drug delivery and therapeutic purposes,[1,2] but also as biorecognition elements in the analytical field, especially for the development of aptasensors, a class of biosensors that uses aptamers for biological recognition.[3-5]

Aptamers are RNA or DNA strands selected through an *in vitro* iterative process, called Systematic Evolution of Ligands by EXponential enrichment (SELEX), which identifies sequences able to recognize with high affinity target molecules through intermolecular interactions such as hydrogen bonds, van der Waals forces, electrostatic interactions, π–π stacking; the formation of an aptamer-target complex can be coupled to conformational changes in the target, the aptamer, or both.[6] Since the advent of SELEX in the early 1990s, hundreds of aptamers have been selected for different target molecules, such as proteins, small organic molecules and even ions, resulting in a proliferation of published studies dealing with the use of aptamers for analytical purposes.[4, 7-10]

Despite the large number of aptamers selected for different targets, nowadays their use is mainly focused on the development of biosensors, with few applications for separation techniques[11,12] such as affinity chromatography, electrochromatography, and affinity capillary electrophoresis, and for sample treatment techniques. The combination of these bioreceptors with magnetic micro- and nanomaterials, which is extensively used in the design of biosensing strategies,[3,13-15] could be useful also to devise selective sample treatment methods, for example magnetic solid-phase extraction (MSPE).[3,15-17]

In the face of an initial enthusiasm for aptamers as a highly promising alternative to antibodies, some recent articles have

addressed critical aspects and challenges concerning their use as bioreceptors, focusing on the affinity and selectivity/specificity of the interaction especially in real matrices, highlighting the need to study the experimental factors influencing aptamer/target interaction.[3,4,7] In this context, an increasing number of articles have raised criticisms regarding the real analytical potentialities of aptamers, providing strong evidence that some aptamers, although widely used in different analytical setups and sensing configurations, are not suitable for target binding and analytical purposes.[18-21] In 2022, Zhao et al. reviewed few recent works claiming that some aptamers could not bind to their target, encouraging the publication of negative results as well to prevent further misleading in the field of aptamers.[21] They explained how the deletion of segments on the 3' and/or 5' sides from the original sequence regardless the validation of their binding capacity is one of the main reasons of binding failure. In the study of Bottari and coworkers,[18] a multifaceted analytical approach involving isothermal titration calorimetry, native nano-electrospray ionization mass spectrometry and ^{1}H-nuclear magnetic resonance spectroscopy proved that none of the three investigated anti-ampicillin aptamers, extensively used in literature in several detection strategies, shows any specific binding to their intended target. Similarly, it was demonstrated that an arsenic-binding aptamer widely used for detection of As(III) did not show any specific As(III) binding.[20]

In this context, Miller at al. argued how the field of aptamer research is particularly susceptible to irreproducibility of research.[22] The authors reviewed hundreds of publications on aptamers over decades, revealing that 41% of the papers reported unexplained sequence alterations or omitted sequences, and identifying ten common categories of sequence alterations including deletions, substitutions, and additions, among others. Critical aspects that influence interaction of aptamers with target molecules, as well as the possible side effects caused by aptamer interaction with other molecules in real samples due to non-specific binding, were recently discussed by our research group with a focus on the strategies in the use of aptamers conjugated to magnetic micro- and nanobeads as recognition elements in food control:[3] we emphasized the importance of evaluating the non-specific binding of aptamers and investigating the matrix effects of apta-assays to ensure the reliability of aptamers as bioreceptors.

On this basis, we reached the conclusion that there is an urgent need to (i) fill the gap between aptamer selection and reliable analytical applications, (ii) prevent misinterpretation of the real performance of a selected aptamer and (iii) critically investigate the applicability of existing aptamer sequences.

Focusing on the use of aptamers for the development of biosensors, it can be observed that one of the main analytical targets of aptasensors is lysozyme, an enzyme that represents an important biomarker for a variety of diseases and one of the five major allergenic proteins found in egg white. The progress made in lysozyme determination using electrochemical and optical aptasensors, based on the most used DNA aptamers has been recently reviewed.[14] The proposed signal transduction approaches for aptasensors aimed at lysozyme determination mainly rely on (i) competition events using complementary oligosequences, (ii) variation of electrochemical impedance, (iii) variation of the recorded signal due to conformational changes of aptamers after the interaction with the target. It is worth to point out that in the latter case the aptasensor is commonly developed without any characterization of the alleged conformational change.

In addition, the rationale for choosing a particular anti-lysozyme sequence and the binding buffer for the aptasensor development is not clear in the literature, which should be done in relation to the specific assay set-up, the buffer used in the SELEX selection and the real matrix. Furthermore, for the biorecognition event, even for the same aptamer, the published works often report the use of buffers, different in terms of nature, concentration of salts and divalent cations, pH value, regardless of the one used for SELEX selection.[23-27] To the best of our knowledge, the only study in which two anti-lysozyme aptamers were compared for the development of an aptasensor for lysozyme determination was published by Ocaña et al.[26]

With the final aim of developing innovative sample treatment strategies and a novel competitive aptasensor based on aptamer-modified magnetic beads for lysozyme determination, in the present work a multi-technique approach was devised to get further insights into the binding performance of the DNA anti-lysozyme aptamers commonly used in literature. For this purpose, we devised and applied a magneto-electrochemical apta-assay, circular dichroism spectroscopy, fluorescence spectroscopy and asymmetrical flow field-flow fractionation with UV detection. Randomly scrambled sequences and a 40-mer thymine sequence (PolyT40) were used as negative controls to assess the sequence specificity of the interaction. The anti-lysozyme RNA aptamer selected by SELEX was also considered in the study as a control.[28]

EXPERIMENTAL SECTION

Chemicals and solutions. A detailed description of all chemicals and solutions is provided in the Supporting Information.

Aptamers. The DNA and RNA sequences, reported in Table S1, were obtained by Biomers.net (Ulm, Germany) and Metabion (Carlo Erba, Milan, Italy) (custom synthesis), and different end-modifications were introduced depending on the experiment type. In particular, an aminolink-C6 modification was introduced to enable crosslinking with carboxylic groups on the surface of the magnetic beads (MBs), while conjugation with cyanine-3 (Cy3) permitted to study aptamer loading on MBs through fluorescence spectroscopy.

In addition, two 20-mer DNA sequences complementary to A40 and A80, respectively, were labelled at 3' end with biotin (Biomers.net, Ulm, Germany).

Magneto-electrochemical apta-assay. Single Walled Carbon Nanotubes Screen-Printed Electrodes (SWCNT-SPEs) and magnetic support for Screen-Printed Electrodes were purchased from Metrohm Italiana Srl (Origgio, Varese, Italy). Aptamer immobilization on MBs is described in the Supporting Information. Aptamer-modified MBs were incubated with 200 µL of lysozyme solution in the binding buffer (PBS-Mg^{2+}, TRIS saline or Tris Glycine Potassium (TGK)) for 1 hour under shaking (1500 rpm) at 26 °C, then washed with 100 µL of binding buffer. Afterwards, MBs were suspended in 200 µL of 10 µg mL^{-1} Strep-ALP in TRIS buffer, containing 5 mg mL^{-1} BSA, and incubated for 15 min under shaking at 26 °C, 1500 rpm; then, MBs were washed with 100 µL of TRIS-T buffer and twice with 100 µL of TRIS buffer. MBs were then separated from buffer and suspended in 50 µL of HQDP solution (1 mg mL^{-1} in TRIS buffer, pH 9.8). After 6 min of incubation, the

suspension was drop-casted on the surface of a SWCNT-SPE, mounted on the magnetic support for confining the MBs on the working electrode surface. Differential Pulse Voltammetry (DPV) measurements were carried out using a PGSTAT204 potentiostat (Metrohm Autolab), by setting the following parameters: potential range -0.5 to 0.2 V; scan rate 12.6 mV s^{-1}; Step 5 mV; Modulation amplitude 50 mV; Modulation time 0.1 s; interval time 0.4 s. Data acquisition and processing was conducted using NOVA 2.1.6 software.

A 40-mer DNA reference probe consisting only of thymine bases (PolyT40) was used as blank reference.

Circular dichroism spectroscopy. Circular dichroism (CD) experiments were performed using a JASCO J-715 spectropolarimeter thermostated by a Peltier unit set at 26 °C using a 1 mm pathlength Suprasil™ quartz cuvette (volume 150 µL). 10 µM solutions of aptamer and lysozyme were prepared separately. Aptamer-protein mixtures were obtained by mixing aptamer and protein solutions in a 1:1 ratio, obtaining a final concentration of 5 µM for each species. Spectra were acquired in the 200-320 nm range for sample in PBS-Mg^{2+} buffer, and in the 210-300 nm range for those in TGK and TRIS saline buffers. All the spectra were recorded through a continuous scan performed at 50 nm min^{-1} rate, with a data pitch of 0.2 nm and a data integration time of 8 s. Spectra accumulation was set from 1 to 5 depending on the signal intensity. Upon buffer subtraction, the CD spectra of the experimental mixtures were compared with the algebraic sum of the spectra of the single components to identify the interaction-induced spectral changes on the aptamer, the protein, or both. Aptamer thermal melting was performed by heating the aptamer solution up to 90 °C. The solution was then maintained at 90 °C for 1 min, followed by cooling to room temperature to check process reversibility.

Fluorescence titration. Emission spectra were recorded on an Edinburgh FLS1000 fluorimeter using a 1 cm pathlength Suprasil™ quartz cuvette (volume 100 µL). The protein was titrated with the aptamer; in detail, lysozyme was diluted in cuvette to reach 1 µM as final concentration. Then, increasing concentrations of aptamer were progressively added. The same procedure was carried out in absence of the protein (blank procedure). Every spectrum was subtracted from the corresponding blank and divided by dilution factor. Protein tryptophans (Trp) were selectively excited at 298 nm and emission spectra were collected from 310 to 550 nm. Excitation and emission bandwidth were set at 3.00 and 2.00 nm, respectively, with 1 nm data pitch. All the spectra were acquired with 1 repeat, dwell time 0.5 s.

Data analysis and titration fitting to a binding isotherm function were carried out using MATLAB R2020b.

Asymmetrical flow field-flow fractionation-UV analysis. The asymmetrical flow field-flow fractionation system coupled to UV detector (AF4-UV) consisted of a 1100 Series HPLC system (Agilent Technologies, Palo Alto, CA) connected to an Eclipse 3 module (Wyatt Technology Europe, Dernbach, Germany) to control AF4 flow rates and operations. The AF4 channel was a Mini Channel (Wyatt Technology Europe) with a regenerated cellulose membrane (Nadir) (molecular weight cut-off: 5 kDa) and a channel spacer thickness of 350 µm. Online detection of the eluted species was performed using an Agilent 1100 DAD UV/Vis spectrophotometer. AF4-UV analysis was carried on A40, C42, PolyT40 and C80RNA sequences and their respective mixtures with lysozyme using PBS-Mg^{2+} binding buffer as elution medium, as described in our previous work.[29] For the preparation of aptamer-protein mixtures, 10 µL of 5 µM aptamer solution in PBS-Mg^{2+} were mixed with 10 µL of lysozyme solution at different concentrations (5, 10, 25, 50 µM) to obtain aptamer:lysozyme molar ratios of 1:1, 1:2, 1:5 and 1:10. Ratios of 2:1, 4:1, 7:1 and 10:1 were also investigated in the case of C80RNA. The percentage of bound aptamer was expressed as $\%(I_{\text{apt alone}} - I_{\text{apt mix}})/I_{\text{apt alone}}$. Data fitting to a binding isotherm function was carried out using MATLAB R2020b.

RESULTS AND DISCUSSION

Identification of Anti-Lysozyme Aptamers under Study. The first step in the development of novel analytical strategies for enrichment or determination of lysozyme, such as aptamer-based MSPE or aptasensors, is the choice of the anti-lysozyme aptamer. The present work has focused on the most commonly used anti-lysozyme DNA aptamers, namely A80, C80 and the corresponding truncated sequences A40, C42 and C30 (see Table S1).[14,24,26,27,30] It is worth noting that C80 is the DNA analog of the SELEX-selected RNA aptamer (C80RNA) reported in literature and that RNA-to-DNA conversion is reported to possibly lead to result inconsistencies.[19, 22]

Considering that DNA has higher intrinsic stability and remarkably lower costs than RNA,[31] the use of DNA aptamers is preferable for developing analytical devices; in fact, most analytical strategies based on anti-lysozyme aptamers involve DNA aptamers. Sequence-selectivity was assessed using unrelated and scrambled oligonucleotide sequences as negative controls.[3] For this purpose, since the SELEX process relies on a sequence library with constant regions flanking a central random region, randomized A80R and C80R were designed to reproduce the same flanking region of A80 and C80, respectively, while randomizing the central one. Furthermore, the PolyT40 polythymine sequence was used both as a blank reference and as a negative control, while C80RNA was investigated as a positive control, with respect to the corresponding DNA analogues.

Based on the current literature, it is very difficult to rationalize the choice of the aptamer and the optimal binding conditions for the development of an analytical approach aimed at lysozyme determination. The issue arises from the variability of experimental conditions reported in the literature for the development of anti-lysozyme aptamer-based sensing strategies in terms of buffer composition, identity and concentration of monovalent and divalent cations and pH values; all of these parameters are able to greatly affect the structure and, therefore, the binding capabilities of aptamers. In this context, the present work was initially aimed at devising a strategy useful to support the selection of the anti-lysozyme DNA aptamer to be immobilized on the surface of MBs as well as to evaluate the effect of the buffer nature on lysozyme recognition. In particular, chemically biotinylated lysozyme was prepared as a model protein to simulate the behavior of the target protein in a magneto-electrochemical apta-assay based on MBs. This platform could also be useful to directly evaluate the effect of different experimental conditions in terms of the nature of the binding buffer, pH, ionic strength, and to study the sequence selectivity of the interaction. The low performance we observed for MBs modified with anti-lysozyme DNA aptamer for target binding motivated us to focus our research activities on a multi-technique characterization of aptamer-lysozyme interaction by circular dichroism, fluorescence spectroscopy and field-flow fractionation.

Magneto electrochemical apta-assay setup. For the assessment of the aptamer-lysozyme interaction a MBs-based electrochemical assay was devised in order to record a signal directly ascribable to the binding event, unlike what happens for assays based on conformational changes or competition events for which the signal is indirectly associated with the aptamer-target interaction. The assay relies on functionalized 5'-aminolink C6 aptamer as a receptor immobilized on carboxyl magnetic beads and on biotinylated lysozyme as a target protein (Figure S1). The presence of biotin labels on lysozyme was necessary to enable the electrochemical reading of the assay which involved the use of the conjugated Strep-ALP for the electrochemical reading. Strep-ALP binds to the biotinylated protein interacting with the aptamer while ALP catalyses the dephosphorylation of the non-electroactive enzyme substrate HQDP to electroactive HQ, thus allowing its oxidation to quinone (Q) via DPV scan and yielding a signal proportional to the amount of interacting target species.

The preliminary study of the immobilization of the aptamer on MBs and the biotinylation of lysozyme was carried out as described in the following paragraphs.

Study of the aptamer immobilization on MBs. The aptamer having a C6 amino group at 5' end was covalently bound to the carboxylated magnetic beads through a common EDC/NHS crosslinking reaction, followed by quenching with ethanolamine and blocking with BSA. A40 was used as a model. To evaluate the loading of aptamers on MBs, we used a 5'-aminolink C6 A40 labelled with Cy3 at 3'-end. To this aim we acquired the fluorescence spectra of the solutions before and after the immobilization of the labelled aptamer on MBs. The differential comparison of the fluorescence emission allowed us to assess the saturation of the active functionalities of the MBs for a A40 concentration higher than 2 µM, corresponding to 542 ± 25 pmol mg^{-1} beads of immobilized aptamer. The conformational freedom of the immobilized aptamer was investigated by reacting A40-functionalized MBs with a 2 µM single strand 20-mer DNA, complementary to a A40 moiety and labelled with biotin at the 3' end. Subsequent incubation with the Strep-ALP conjugate and signal readout in the presence of HQDP substrate gave results confirming the efficiency of complementary based pairing (Figure S2), where DPV signals recorded with functionalized and not-functionalized MBs are compared. The high voltammetric signal recorded in the presence of A40 confirmed the proper immobilization of the aptamer on the magnetic support, whereas the flat signal obtained with non-functionalized MBs assured us the absence of non-specific adsorption of the Strep-ALP conjugate on the micromagnetic substrate.

The efficacy of modifying MBs with longer sequences was confirmed by performing the same pairing experiments with A80, thus obtaining results comparable to A40.

Lysozyme biotinylation. Biotinylation of lysozyme was carried out by a commercial kit using NHS-PEG4-biotin as biotinylating agent, as described in the Supporting Information. After dialysis aimed at removing not reacted biotinylating reagents and NHS leaving group, biotinylated lysozyme was quantified by spectrophotometric measurements, obtaining a concentration of 206 ± 6 µM. Then, biotinylated lysozyme was further characterized by flow injection analysis-mass spectrometry (FIA-MS). The MS spectrum showed different multi-charge distributions, each related to lysozyme species with different degrees of biotinylation; the most abundant charge states were +9, +10 and +11 (Figure S3).

It is also worth noting the absence of peaks associated to unmodified lysozyme, free biotinylating agent and NHS, indicating effective biotinylation and dialysis. Based on the sum of the most abundant multicharged states for each lysozyme species, it was calculated that the mean value of number of biotin copies per lysozyme molecule was 3.4 ± 0.1. In addition, the acquisition of the CD spectra for both native and biotinylated lysozyme allowed us to verify that the protein conformation remained unchanged after the introduction of the biotin molecules (Figure S4).

Study of the aptamer/lysozyme interaction by the electrochemical assay. Experiments aimed at evaluating the interaction with the lysozyme were performed by studying the binding capacity of MB-immobilized aptamers to the target protein. To this end, the concentration of biotinylated lysozyme was fixed at 500 nM and the MBs were functionalized with different aptamers (Table S1). PolyT40 was used as a blank reference: its immobilization on the MBs allowed us to simulate the condition of MBs modified by a putative non-interacting sequence. The same experiments were carried out in TRIS saline and in PBS-Mg^{2+} buffers, which are the most commonly used working buffers for anti-lysozyme aptamers; in addition, TRIS saline buffer is the C80RNA aptamer selection buffer.[28]

Figure 1 shows the comparison between the signals obtained from all the investigated aptamers, also indicating the averaged signal for PolyT40.

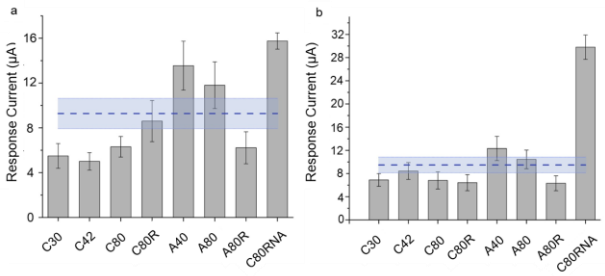

Figure 1. Comparison of DPV signals from magneto-electrochemical apta-assays between the aptamers studied in (a) PBS-Mg^{2+} and (b) TRIS saline buffers (n=3). The dashed blue lines and light-blue boxes correspond respectively to the mean and standard deviation of the signals resulting from the immobilization of PolyT40 used as a blank reference.

For DNA sequences, although a stronger interaction was evidenced for the A40 and A80 aptamers, the relatively high signal observed even with the PolyT40-functionalized MBs highlighted an interaction not related to the sequence. In the case of A40 in PBS-Mg^{2+} the signal was significantly different (p<0.05) than PolyT40.

Furthermore, the high dispersion of the signals can be attributed to the non-specificity of the interactions. On the other hand, in both PBS-Mg^{2+} and TRIS saline buffers, C80RNA gave a significantly different signal with respect to PolyT40, with RSD% lower than 8%. In addition, in the SELEX-selection buffer (TRIS saline) the signal of C80RNA was 4.4 times that of the analogous DNA-based aptamer (i.e. C80). On the basis of these findings, further investigations were carried out on a small number of sequences, focusing the attention on the most widely used

aptamers for the lysozyme determination, i.e. C42 and A40, derived from truncation of full-length sequences selected by different SELEX experiments, by maintaining PolyT40 - as a blank reference and negative control - as well as C80RNA.
At first, we carried out the electrochemical assay for C42, A40, PolyT40 and C80RNA sequences in TGK, which is the buffer used for the selection of the A80 aptamer. The results demonstrated the effect of buffer composition on absolute and relative signals. As can be observed, for DNA aptamers the signals in TGK were approximately three times higher than those recorded in PBS-Mg^{2+} and TRIS saline buffers, probably due to the absence of salts which act as DNA counterions, also causing a levelling effect on the signal intensity for all the sequences (Figure 2).

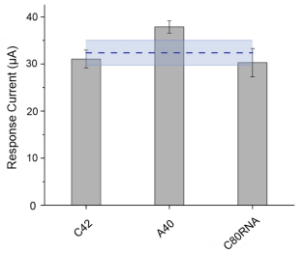

Figure 2. Comparison of DPV signals from magneto-electrochemical apta-assays for A40, C42, C80RNA in TGK buffer (n=3). The dashed blue line and the light blue box correspond respectively to the mean and standard deviation of the signals resulting from the immobilization of PolyT40 used as a blank reference.

Conformational characterization by circular dichroism spectroscopy. Based on these results, which highlighted a different behavior of the aptamers as a function of the composition of the buffer, circular dichroism measurements were performed to evaluate the influence of the buffer on the secondary structure of the aptamers and therefore also on the affinity for the target. For this purpose, we acquired CD spectra in PBS-Mg^{2+} and TGK buffers, since they have been shown to provide for DNA aptamers the greatest signal differences between the sequences and the highest intensities, respectively. The CD spectra highlighted the different conformations of the C42 and A40 sequences in the two buffers; in particular, a shift of the peak and an inflection point shift were observed for A40 (Figure 3a) and C42 sequences (Figure 3b), respectively; furthermore, the influence of the buffer was observed on C80RNA conformation as well (Figure 3c), whereas PolyT40 resulted to be unaffected by buffer composition (Figure 3d). These findings confirmed an effect of the buffer on the aptamer structure, highlighting that the choice of the binding buffer needs rationalization for the development of aptamer-based analytical methods. Measurements in CD were also performed to study the effect of denaturation on the conformation of the investigated aptamers and to study the interactions between aptamers and target protein. Since the aptamer can adopt different conformations in solutions, several studies in the literature suggest performing a thermal melting followed by slow cooling before use, thus homogenizing aptamer folding pathways and minimizing batch-to batch variation.[19,23] This aspect was investigated by recording CD spectra of A40 and C42 before and after denaturation at 90 °C. From the comparison of the CD spectra, it was observed that for both aptamers (A40 and C42) denaturation and subsequent refolding did not cause a conformational change (Figure S5).

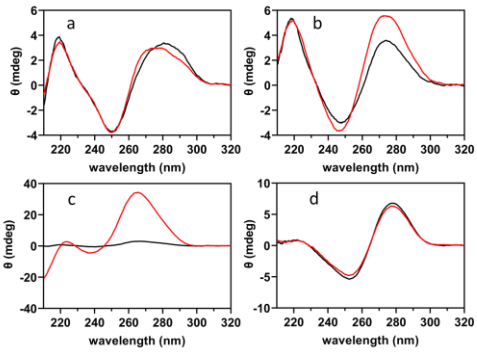

Figure 3. Overlay of CD spectra of (a) A40, (b) C42, (c) C80RNA, (d) PolyT40 in PBS-Mg^{2+} (red) and TGK (black) buffers. Aptamer concentration: 10 μM.

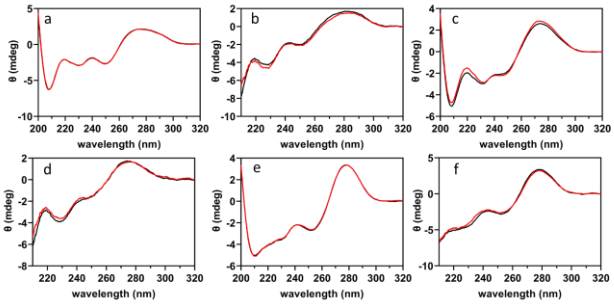

Figure 4. CD spectra of the equimolar mixture (red) and the algebraic sum (black) of lysozyme with A40 aptamer in (a) PBS-Mg^{2+} and (b) TGK buffers; with C42 aptamer in (c) PBS-Mg^{2+} and (d) TGK buffers; with PolyT40 in (e) PBS-Mg^{2+} and (f) TGK buffers.

As for the study of the lysozyme/aptamer interaction using CD, the experimental spectrum of an equimolar aptamer:lysozyme mixture was compared with the sum of the spectra of the individual components, as described in the experimental section. As already observed, in the presence of an interaction, a difference between the experimental spectrum and the algebraic sum of the CD spectra are expected if the interaction causes conformational changes on the lysozyme, the aptamer, or both.[32] From the results shown in Figure 4, it is noted that no differences were observed in PBS-Mg^{2+} buffer, and minimal differences were observed in TGK buffer, which however cannot be considered as significant. It can be concluded that in this case the CD analysis did not allow to demonstrate a lysozyme/aptamer interaction; however, this does not exclude that an interaction may exist, but in this case the binding is not associated with a conformational change of either the protein or the aptamer.
The same CD experiment was carried out with C80RNA in TRIS saline (the binding buffer used in SELEX), PBS-Mg^{2+} and TGK. A difference in the experimental spectrum for the lysozyme/aptamer mixture compared to the algebraic sum spectrum was observed both in TRIS saline, confirming protein binding, and in PBS-Mg^{2+}, but not in TGK buffer (Figure 5). These findings, in accordance with the results from the electrochemical assay, proved the possibility of exploiting CD to evaluate the conformational changes, likely arising from the aptamer, upon complex formation.

Furthermore, the CD results suggest that the development of aptasensing strategies based on target-induced conformational change of the aptamer[14] would benefit from the preliminary CD investigation for validating the sensor principle of detection, taking into account that CD allows to assess potential conformational changes that occur after binding events.

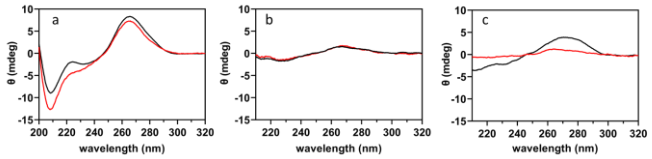

Figure 5. CD spectra of the equimolar mixture (red) and the algebraic sum (black) of lysozyme with C80RNA aptamer in (a) PBS-Mg^{2+}, (b) TGK and (c) TRIS saline.

Binding assays by fluorescence titration. The aptamer-lysozyme interaction was also studied for A40, C42 and PolyT40 in PBS-Mg^{2+} and TGK buffers using fluorescence spectroscopy in order to measure the molecular binding by determining a binding curve and calculate the K_d constant.

The intrinsic fluorescence of lysozyme was exploited, avoiding the use of fluorescent tags, by selectively exciting Trp residues at 298 nm.

For all the DNA aptamers analyzed we observed a similar behavior: the lysozyme fluorescence emission has a maximum at 337 nm and decreases in intensity with increasing aptamer concentration (Figures S6 and S7), possibly related to a static fluorescence quenching or a chemical environmental change of Trp caused by interaction with the aptamer.

Figure 6 shows the binding curves for A40, C42 and PolyT40 aptamers in PBS-Mg^{2+} and TGK buffers; the calculated K_d values are reported in Table 1.

The results highlight that the interaction appears to be non-sequence specific. In addition, the K_d values in PBS-Mg^{2+} are in agreement with those reported by other authors in 20 mM TRIS when the NaCl concentration is increased up to 100 mM:[33] in that study, the authors proved that the affinity of C42 and other DNA analogs of RNA aptamers, among those reported by Kirby et al.,[34] is not strictly sequence dependent, but rather it is mediated by non-specific interactions.

We also carried out the same fluorescence experiments on C80RNA in different buffers, but the results showed variability in binding behavior that precluded the determination of dissociation constants, while revealing an interaction. For this longer RNA-based sequence, this would suggest a more complex binding scenario with possible more binding sites, with similar or partially overlapping affinities. In fact, Trp fluorescence emission, giving a measure of local changes on the protein, could give different signal changes depending on the binding mode and stoichiometry: on one side this technique could offer precious structural insights in case of a single, well defined complex structures, but in case of binding heterogeneity it can lose a direct proportionality between the signal and the concentration of the complex.

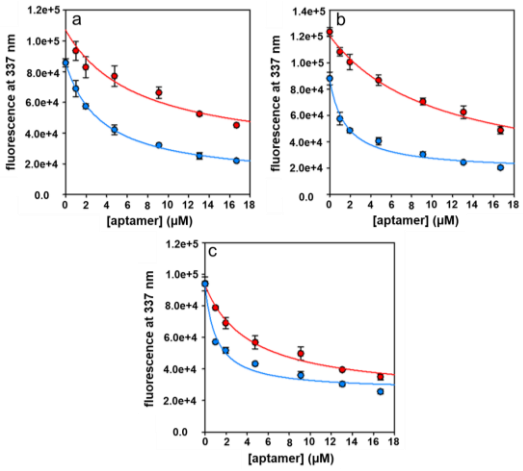

Figure 6. Binding curves from fluorescence titration for (a) A40, (b) C42 and (c) PolyT40 in PBS-Mg^{2+} (red) and TGK buffers (blue) (n=3).

Table 1. Dissociation constant (K_d) for A40, C42 and PolyT40 in PBS-Mg^{2+} and TGK buffers.

	K_d (μM)	
	PBS-Mg^{2+}	TGK
A40	7.0 ± 4.0	3.5 ± 0.3
C42	10.5 ± 3.9	1.6 ± 0.4
PolyT40	4.3 ± 1.1	1.1 ± 0.3

Binding assays by asymmetrical flow field-flow fractionation-UV. To gain further insights into the molecular principles of lysozyme-aptamer interactions, asymmetrical flow field-flow fractionation was used, since it represents a gentle separation and characterization method, where unspecific interactions are reduced to a minimum working in representative conditions, such as binding buffer and biocompatible media. In comparison with other size-based separation techniques such as size exclusion chromatography, it preserves structural integrity, molecular conformation, conformational arrangement of particles and macromolecules in suspension (native separation) as well as activity during analysis.[35-37] This technique can also overcome the observed limit of Trp fluorescence in characterizing C80RNA binding affinity. Parallel to the present work, we have recently developed a AF4-UV method to get insights into interactions between aptamers and proteins;[29] in that study, all the anti-lysozyme DNA aptamers investigated in the present work, except C42 and the PolyT40 sequence, have been screened in PBS-Mg^{2+} and the results obtained confirmed a modest affinity and a behaviour of C80 and C30 comparable to that of the negative controls (scrambled sequences). In order to complete the characterization, in the present work the AF4-UV method was applied to evaluate the percentage of bound aptamer at different lysozyme concentrations also for C42, PolyT40 and C80RNA.

From the results reported in Figure 7a, it can be concluded that the behaviour of C42 is comparable to that of the negative control. The reader is referred to Marassi et al.[29] for the results of A40. The C80RNA aptamer showed the highest affinity for lysozyme allowing to calculate a fraction of bound aptamer at aptamer:lysozyme ratios higher than 1:1, corresponding to a decrease in lysozyme concentration. As shown in Figure 7b, it was possible to construct a binding curve for C80RNA in PBS-Mg^{2+}, giving a K_d of 1.7 ± 0.5 μM; this result confirms also the

potential of AF4 to quantitatively measure binding behaviour of aptamers.

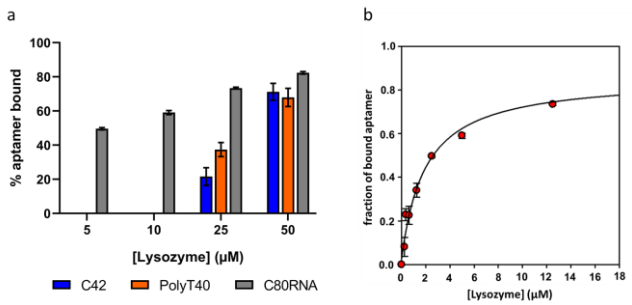

Figure 7. (a) Percentage of bound aptamer for C42, PolyT40 and C80RNA in PBS-Mg^{2+} (n = 3). (b) Binding curve from AF4-UV for C80RNA in PBS-Mg^{2+} (n=3).

As for the poor performance of C42, the behaviour of this aptamer can be attributed to the fact that researchers attempted to make a DNA version of a RNA anti-lysozyme aptamer, probably due to a misinterpretation of the original table listing the template DNA sequences.[22,28,34], followed also by non-rationalized sequence truncation. It has been shown that RNA and DNA versions of an identical sequence can exhibit different behaviour, not interacting with the same ligands.[21,33,38,39]

CONCLUSIONS

The scientific community has recently become aware that greater methodological rigor is needed to evaluate the real analytical potential of aptamers. According to literature,[18,20,40] multi-technique strategies are essential to obtain a reliable characterization of aptamer/target systems and avoid inconsistency of results. For the characterization and validation of the aptamer/target interaction, multiple technique combinations have to be properly tuned, involving methods that (i) match or simulate the final aptamer application, (ii) rationalize and validate the aptasensor mechanism. In the present study, a magneto apta-assay was well suited to the final aim of developing magnetic beads-based analytical approaches and was used to compare the performance of different aptamer candidates, including negative and positive controls. Taking into account the influence of the aptamer immobilization and aptamer/target labelling on the binding event, label-free techniques and in-solution methods, such as intrinsic fluorescence measurements and flow field-flow fractionation proposed here, should be included for candidates screening, selection and binding event characterization in native conditions. In addition, if the final analytical method is based on a target-induced conformational change of the aptamer, this mechanism can be properly validated by circular dichroism spectroscopy.

Taking into account that lysozyme is one of the main analytical targets of aptasensors, the present work represents the first study aimed at investigating, through a multi-technique approach, the binding properties of different anti-lysozyme DNA aptamers widely used in the literature for the development of analytical methods. In addition to showing a lower than expected aptamer/protein affinity, the investigated DNA aptamers behaved similarly to the negative controls, *i.e.* randomized and polythymine sequences, allowing to clearly demonstrate that the oligonucleotides can interact with lysozyme regardless of their sequence.

This work moves in the direction of a growing list of published articles calling for adequate and rigorous testing of candidate aptamers with appropriate controls and exploring different binding conditions, recognized as the unique way to advance the aptamer field within the analytical scenario.

ASSOCIATED CONTENT

Supporting Information

The Supporting Information is available free of charge on the ACS Publications website.

Supporting experimental section, aptamer sequences, scheme of the magneto-electrochemical apta-assay, DPV voltammogram from aptamer-modified magnetic beads, ESI(+)-MS spectrum of biotinylated lysozyme; CD spectra of lysozyme and biotinylated lysozyme, CD spectra of A40 and C42 after denaturation and refolding; fluorescence titration curves of lysozyme with A40, C42 and PolyT40 sequence in PBS-Mg^{2+} and TGK buffers (PDF).

AUTHOR INFORMATION

Corresponding Author

* **Monica Mattarozzi** - Department of Chemistry, Life Sciences and Environmental Sustainability, University of Parma, Parco Area delle Scienze 17/A, 43124, Parma, Italy; Interdepartmental Center SITEIA.PARMA, University of Parma, Parco Area delle Scienze 181/A, 43124, Parma, Italy; orcid.org/0000-0002-6766-4616; Email: monica.mattarozzi@unipr.it

Author Contributions

All authors have given approval to the final version of the manuscript.

Notes

The authors declare no competing financial interest.

ACKNOWLEDGMENT

This work was supported by the project PRIN 2017 (Progetti di Ricerca di Rilevante Interesse Nazionale) grant N. 2017YER72K funded by the MIUR (Italian Ministry for Education, University and Research).

This work has also benefited from the framework of the COMP-HUB Initiative, funded by the 'Departments of Excellence' program of the Italian Ministry for Education, University and Research (MIUR, 2018-2022).

REFERENCES

(1) He, F.; Wen, N.; Xiao, D.; Yan, J.; Xiong, H.; Cai, S.; Liu, Z.; Liu, Y. Aptamer-based targeted drug delivery systems: current potential and challenges. *Curr. Med. Chem.* **2020**, *27*, 2189-2219.

(2) Ni, S.; Zhuo, Z.; Pan, Y.; Yu, Y.; Li, F.; Liu, J.; Wang, L.; Wu, X.; Li, D., Wan, Y.; Zhang, L.; Yang, Z.; Zhang, B.-T.; Lu, A.; Zhang, G. Recent progress in aptamer discoveries and modifications for therapeutic applications. *ACS Appl. Mater. Interfaces* **2021**, *13*, 9500-9519.

(3) Mattarozzi, M.; Toma, L.; Bertucci, A.; Giannetto, M.; Careri, M. Aptamer-based assays: strategies in the use of aptamers conjugated to magnetic micro- and nanobeads as recognition elements in food control. *Anal. Bioanal. Chem.* **2022**, *414*, 63-74.

(4) Kalita, J.J.; Sharma, P.; Bora, U. Recent developments in application of nucleic acid aptamer in food safety. *Food Control* **2023**, *145*, 109406.

(5) Liu, L.S.; Wang, F.; Ge, Y.; Lo. P.K. Recent developments in aptasensors for diagnostic applications. *ACS Appl. Mater. Interfaces* **2021**, *13*, 9329-9358.

(6) Kohlberger, M.; Gadermaier, G. SELEX: critical factors and optimization strategies for successful aptamer selection. *Biotechnol. Appl. Biochem.* **2022**, *69*, 1771-1792.

(7) Wu, Y.; Belmonte, I.; Sykes, K.S.; Xiao, Y.; White, R.J. Perspective on the future role of aptamers in analytical chemistry. *Anal. Chem.* **2019**, *91*, 15335-15344.

(8) Kotlarek, D.; Curti, F.; Vorobii, M.; Corradini, R.; Careri, M.; Knoll, W.; Rodriguez-Emmenegger, C.; Dostálek, J. Surface plasmon resonance-based aptasensor for direct monitoring of thrombin in a minimally processed human blood. *Sens. Actuators B: Chem.* **2020**, *320*, 128380.

(9) Zon, G. Recent advances in aptamer applications for analytical biochemistry. *Anal Biochem.* **2022**, *644*, 113894.

(10) Rodrigues, T.; Curti, F.; Leroux, Y.R., Barras, A.; Pagneux, Q.; Happy, H.; Kleber, C.; Boukherroub, R.; Hasler, R.; Volpi, S.; Careri, M.; Corradini, R.; Szunerits, S.; Knoll, W. Discovery of a Peptide Nucleic Acid (PNA) aptamer for cardiac troponin I: Substituting DNA with neutral PNA maintains picomolar affinity and improves performances for electronic sensing with graphene field-effect transistors (gFET). *Nano Today* **2023**, *50*, 101840.

(11) Ravelet, C.; Grosset, C.; Peyrin, E. Liquid chromatography, electrochromatography and capillary electrophoresis applications of DNA and RNA aptamers. J. Chromatogr. A **2006**, *1117*, 1-10.

(12) Zhao, Q.; Wu, M.; Le Chris, X.; Li, X.-F. Applications of aptamer affinity chromatography. *Trends Anal. Chem.* **2012**, *41*, 46-57.

(13) Mattarozzi, M.; Giannetto, M.; Careri, M. Electrochemical immunomagnetic assay as biosensing strategy for determination of ovarian cancer antigen HE4 in human serum. Talanta **2020**, *217*, 120991.

(14) Melinte, G.; Selvolini, G.; Cristea, C.; Marrazza, G. Aptasensors for lysozyme detection: recent advances. *Talanta* **2021**, *226*, 122169.

(15) Modh, H.; Scheper, T.; Walter, J.-G. Aptamer-modified magnetic beads in biosensing. *Sensors* **2018**, *18*, 1041.

(16) Pichon, V.; Brothier, F.; Combès, A. Aptamer-based-sorbents for sample treatment-a review. *Anal. Bioanal. Chem.* **2015**, *407*, 681-698.

(17) Vergara-Barberán, M.; Lerma-García, M.J.; Moga, A.; Carrasco-Correa, E.J.; Martínez-Pérez-Cejuela, H.; Beneito-Cambra, M.; Simó-Alfonso, E.F.; Herrero-Martínez, J.M. Recent advances in aptamer-based miniaturized extraction approaches in food analysis. *Trends Anal. Chem.* **2021**, *138*, 116230.

(18) Bottari, F.; Daems, E.; de Vries, A.-M.; Van Wielendaele, P.; Trashin, S.; Blust, R.; Sobott, F.; Madder, A.; Martins, J.C.; De Wael, K. Do aptamers always bind? the need for a multifaceted analytical approach when demonstrating binding affinity between aptamer and low molecular weight compounds. *J. Am. Chem. Soc.* **2020**, *142*, 19622-19630.

(19) Cho, E.J.; Lee, J.-W.; Ellington, A.D. Applications of aptamers as sensors. *Annu. Rev. Anal. Chem.* **2009**, *2*, 241-264.

(20) Zong, C.; Liu, J. The arsenic-binding aptamer cannot bind arsenic: critical evaluation of aptamer selection and binding. *Anal. Chem.* **2019**, *91*, 10887-10893.

(21) Zhao, Y.; Yavari, K.; Liu, J. Critical evaluation of aptamer binding for biosensor designs. *Trends Anal. Chem.* **2022**, *146*, 116480.

(22) Miller, A.A.; Rao, A.S.; Nelakanti, S.R.; Kujalowicz, C.; Shi, T.; Rodriguez, T.; Ellington, A.D.; Stovall, G.M. Systematic review of aptamer sequence reporting in the literature reveals widespread unexplained sequence alterations. *Anal. Chem.* **2022**, *94*, 7731-7737.

(23) Zhao, L.; Li, L.; Zhu, C.; Ghulam, M.; Qu, F. pH-responsive polymer assisted aptamer functionalized magnetic nanoparticles for specific recognition and adsorption of proteins. *Anal. Chim. Acta* **2020**, *1097*, 161-168.

(24) Lin, Y.; Sun, Y.; Dai, Y.; Zhu, X.; Liu, H.; Han, R.; Gao, D.; C. Luo, Wang, X. A chemiluminescence assay for determination of lysozyme based on the use of magnetic alginate-aptamer composition and hemin@HKUST-1. *Microchimica Acta* **2020**, *187*, 281.

(25) Mihai, I.; Vezeanu, A.; Polonschii, C., Albu, C.; Radu, G.-L.; Vasilescu, A. Label-free detection of lysozyme in wines using an aptamer based biosensor and SPR detection. *Sensors Actuat. B* **2015**, *206*, 198-204.

(26) Ocaña, C.; Hayat, A.; Mishra, R.K.; Vasilescu, A.; Del Valle, M.; Marty, J.-L. Label free aptasensor for lysozyme detection: A comparison of the analytical performance of two aptamers. *Bioelectrochemistry* **2015**, *105*, 72-77.

(27) Rezaei, B.; Jamei, H.R.; Ensafi, A.A. An ultrasensitive and selective electrochemical aptasensor based on rGO-MWCNTs/Chitosan/carbon quantum dot for the detection of lysozyme. *Biosens. Bioelectron.* **2018**, *115*, 37-44.

(28) Cox, J.C.; Ellington, A.D. Automated Selection of Anti-Protein Aptamers. *Bioorg. Med. Chem.* **2001**, *9*, 2525-2531.

(29) Marassi, V.; Mattarozzi, M.; Toma, L.; Giordani, S.; Ronda, L.; Roda, B.; Zattoni, A.; Reschiglian, P.; Careri, M. FFF-based high-throughput sequence shortlisting to support the development of aptamer-based analytical strategies. *Anal. Bioanal. Chem.* **2022**, *414*, 5519-5527.

(30) Tran, D.T.; Janssen, K.P.F.; Pollet, J.; Lammertyn, E.; Anné, J.; Van Schepdael, A., Lammertyn, J. Selection and characterization of DNA aptamers for egg white lysozyme. *Molecules* **2010**, *15*, 1127-1140.

(31) Amero, P.; Lokesh, G.L.R.; Chaudhari, R.R.; Cardenas-Zuniga, R.; Schubert, T., Attia, Y.M., Montalvo-Gonzalez, E., Elsayed, A.M., Ivan, C., Wang, Z., Cristini, V.; de Franciscis, V.; Zhang, S., Volk, D.E.; Mitra, R.; Rodriguez-Aguayo, C.; Sood, A.K.; Lopez-Berestein, G. Conversion of RNA aptamer into modified DNA aptamers provides for prolonged stability and enhanced antitumor activity. *J. Am. Chem. Soc.* **2021**, *143*, 7655-7670.

(32) Ronda, L.; Tonelli, A.; Sogne, E.; Autiero, I.; Spyrakis, F.; Pellegrino, S.; Abbiati, G.; Maffioli, E.; Schulte, C.; Piano, R.; Cozzini, P.; Mozzarelli, A.; Bettati, S.; Clerici, F.; Milani, P.; Lenardi, C.; Tedeschi, G.; Gelmi M.L. Rational Design of a User-Friendly Aptamer/Peptide-Based Device for the Detection of *Staphylococcus aureus*, *Sensors* **2020**, *20*, 4977.

(33) Potty, A.S.R.; Kourentzi, K.; Fang, H.; Schuck, P.; Willson, R.C. Biophysical characterization of DNA and RNA aptamer interactions with hen egg lysozyme. *Int. J. Biol. Macromol.* **2011**, *48*, 392-397.

(34) Kirby, R.; Cho, E.J.; Gehrke, B.; Bayer, T.; Park, Y.S.; Neikirk, D.P.; McDevitt, J.T.; Ellington, A.D. Aptamer-based sensor arrays for the detection and quantitation of proteins. *Anal. Chem.* **2004**, *76*, 4066-4075.

(35) Ventouri, I.K.; Loeber, S.; Somsen, G.W.; Schoenmakers, P.J.; Astefanei, A. Field-flow fractionation for molecular-interaction studies of labile and complex systems: A critical review. *Anal. Chim. Acta* **2022**, *1193*, 339396.

(36) Marassi, V.; Giordani, S.; Reschiglian, P.; Roda, B.; Zattoni, A. Tracking Heme-Protein interactions in healthy and pathological human serum in native conditions by miniaturized FFF-multidetection. *Appl. Sci.* **2022**, *12*, 6762.

(37) Marassi, V.; Zanoni, I.; Ortelli, S.; Giordani, S.; Reschiglian, P.; Roda, B.; Zattoni, A.; Ravagli, C.; Cappiello, L.; Baldi, G.; Costa, A.L.; Blosi, M. Native study of the behaviour of magnetite nanoparticles for hyperthermia treatment during the initial moments of intravenous administration. *Pharmaceutics* **2022**, *14*, 2810.

(38) Ellington, A.D.; Szostak, J.W. Selection in vitro of single-stranded DNA molecules that fold into specific ligand-binding structures. Nature **1992**, *355*, 850-852.

(39) Hou, Y.; Hou, J.; Liu, X. Comparison of two DNA aptamers for dopamine using homogeneous binding assays. *ChemBioChem* **2021**, *22*, 1948-1954.

(40) McKeague, M.; De Girolamo, A.; Valenzano, S.; Pascale, M.; Ruscito, A.; Velu, R.; Frost, N.R.; Hill, K.; Smith, M.; McConnell, E.M.; DeRosa, M.C. Comprehensive analytical comparison of strategies used for small molecule aptamer evaluation. *Anal. Chem.* **2015**, *87*, 8608-8612.

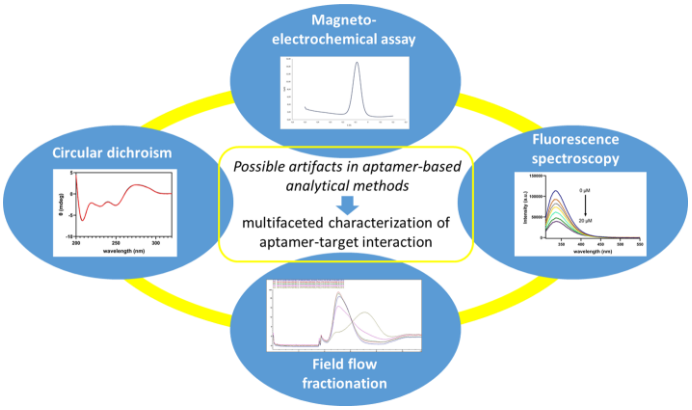
Magneto-electrochemical assay
Circular dichroism
Fluorescence spectroscopy
Field flow fractionation
Possible artifacts in aptamer-based analytical methods
multifaceted characterization of aptamer-target interaction

SUPPORTING INFORMATION

Are aptamers really promising as receptors for analytical purposes? Insights into anti-lysozyme DNA aptamers through a multi-technique study

Lorenzo Toma[a], Monica Mattarozzi[a,b,*], Luca Ronda[c,d], Valentina Marassi[e,f,g], Andrea Zattoni[e,f,g], Simone Fortunati[a,g], Marco Giannetto[a,b,g], Maria Careri[a,b,g]

[a] Department of Chemistry, Life Sciences and Environmental Sustainability, University of Parma, Parco Area delle Scienze 17/A, 43124, Parma, Italy

[b] Interdepartmental Center SITEIA.PARMA, University of Parma, Parco Area delle Scienze 181/A, 43124, Parma, Italy

[c] Department of Medicine and Surgery, University of Parma, Parco Area delle Scienze, 23/A, 43124, Parma, Italy

[d] Institute of Biophysics, CNR, 56124 Pisa, Italy

[e] Department of Chemistry, University of Bologna, Via Selmi 2, 40126, Bologna, Italy

[f] byFlow srl, Bologna, Italy

[g] INBB, National Institute for Biostructures and Biosystems, Rome, Italy

*Corresponding author

Monica Mattarozzi, email: monica.mattarozzi@unipr.it

Table of contents

Supporting experimental section

Chemicals and solutions. Magnesium chloride ($MgCl_2$), ammonium bicarbonate (NH_4HCO_3), L-glycine, Trizma® base, Tween-20, ethanolamine (EA), N-(3-dimethylaminopropyl)-N'-ethylcarbodiimide hydrochloride (EDC), N-hydroxysuccinimide (NHS), bovine serum albumin (BSA), iodoacetamide (IAA), DL-dithiothreitol (DTT), sodium hydroxide, sodium chloride, 4-morpholineethanesulfonic acid monohydrate (MES), hydrochloric acid, formic acid (FA), acetonitrile (ACN), streptavidin-alkaline phosphatase from *Streptomyces avidinii* conjugate (Strep-ALP) and lysozyme from chicken egg white were purchased from Merck (Milan, Italy). Monobasic potassium phosphate (KH_2PO_4), di-potassium hydrogen phosphate (K_2HPO_4), sodium phosphate dibasic dodecahydrate ($Na_2HPO_4 \cdot 12H_2O$), potassium chloride and RNase free water were purchased from Carlo Erba (Cornaredo, Milan, Italy). Hydroquinone diphosphate (HQDP) was provided by Metrohm Italiana (Origgio, Varese, Italy).
Deionized water was obtained by Milli-Q element A10 system (Millipore, San Francisco, CA, USA), and used for buffer solutions preparation.
The composition of the buffer solutions was as follows. MES buffer: 25 mM MES (pH 5); TRIS buffer: 0.1 M Trizma® Base, 5 mM $MgCl_2$ (pH 7.4); TRIS-T buffer: 0.1 M Trizma® Base, 5 mM $MgCl_2$, 0.05% w/v Tween® 20 (pH 7.4); TRIS saline buffer : 20 mM Trizma® Base, 5 mM $MgCl_2$, 0.1 M NaCl (pH 7.4); Phosphate Buffer Saline containing magnesium ions (PBS-Mg^{2+}): 1.5 mM KH_2PO_4, 8 mM Na_2HPO_4, 137 mM NaCl, 2.7 mM KCl, 1 mM $MgCl_2$ (pH 7.4); Phosphate Buffered Saline (PBS) was purchased as dry-blended powder from Thermo Fisher Scientific (Waltham, MA, USA), having the following composition after dissolution: 0.1 M Na_2HPO_4, 0.15M NaCl (pH 7.2); Tris Glycine Potassium (TGK) buffer: 25 mM Trizma® Base, 192 mM L-glycine, 5 mM K_2HPO_4 (pH 8.3).
RNase-free buffers were used in all experiments with the RNA aptamer.
The single stranded DNA sequences were purchased from Biomers.net (Ulm, Germany) whereas C80RNA sequence was from Metabion (Carlo Erba, Milan, Italy). All the oligos were delivered in a dried state, properly aliquoted to avoid repeated freeze/thaw cycles. The resuspension of the lyophilized aliquots was carried out in milli-Q water for the DNA oligos whereas in RNase-free water for C80RNA to reach a 100 μM final concentration as recommended by the supplier. The stock solutions were stored at -20°C.

Lysozyme biotinylation. Lysozyme biotinylation was performed using EZ-Link NHS-PEG4-Biotinylation Kit (Thermo Scientific). Biotinylation reaction was carried out in PBS buffer at 1:5 (lysozyme: biotinylating agent) ratio, for 1 hour at room temperature under gentle stirring. The biotinylated protein was purified by dialysis, using a regenerated cellulose membrane with cut-off of 10 kDa, under gentle stirring for 4 hours, refreshing PBS buffer after 2 hours. After dialysis, the protein solution was centrifuged at 4 °C, 10000 rpm for 10 min and the supernatant was collected.
The concentration of biotinylated lysozyme was quantified by spectrophotometric analysis, using UV-vis/NIR Lambda 750 Perkin Elmer spectrophotometer equipped with a diode array detector. The calibration curve was constructed by analysing four concentration levels of lysozyme at 280 nm, assuming the same molar extinction coefficient for the unmodified and biotinylated protein.

Biotinylation grade was estimated by Flow Injection Analysis (FIA)-Mass Spectrometry (MS) using HPLC Dionex Ultimate 3000 coupled with a linear ion trap (LTQ) mass spectrometer (Thermo Fisher Scientific), equipped with an electrospray (ESI) source, operating in positive polarity. FIA-MS analysis was carried out by injecting 10 µL of sample; three injections of biotinylated lysozyme were performed. A mobile phase consisting of water with 0.1% FA (*v*/*v*) at a flow-rate of 200 µL min^{-1} was used. The conditions were set as follows: electrospray voltage of 3.5 kV, capillary temperature of 200 °C and capillary voltage of 20 V. Mass spectra were acquired in 5 min in full-scan mode (*m/z* 110-2000 range).

Aptamer immobilization on magnetic beads. A volume of 4 µL of stock suspension (2×10^9 beads mL^{-1}, corresponding to approximately 30 mg mL^{-1}) of Dynabeads™ M-270 Carboxylic Acid (Life Technologies Italia–Thermo Fisher Scientific) were diluted in 100 µL of MES buffer. MBs were washed 2 times with MES buffer, then they were suspended in 200 µL of a solution containing EDC and NHS, both at 25 mg mL^{-1}, for 30 min under shaking at 1500 rpm at room temperature using a shaking heater block (Thermomixer®C, Eppendorf). Subsequently, MBs were washed with MES buffer and suspended in a 2 µM aptamer solution. Immobilization time was set to 2 hours, working at 26 °C under shaking (1500 rpm). After MBs washing with 100 µL of MES and 100 µL of TRIS buffer, the functionalized MBs were incubated with 100 µL of EA (50 mM in TRIS buffer) to quench the activated sites for 1 hour under shaking at 1500 rpm. MBs were washed with 100 µL of TRIS-T buffer and 100 µL of binding buffer (PBS-Mg^{2+}, TRIS saline or TGK) for two times, then they were incubated with 200 µL of BSA 0.5% (w/w) as blocking agent for 1 hour at 26 °C, under shaking at 1500 rpm. Finally, MBs were washed twice with 100 µL of binding buffer.
The MB functionalization was studied by using the A40 sequence modified at 3' with Cy3 performing fluorescence measurements (λ_{exc}=555 nm; λ_{em}= 565 nm) with an Edinburgh FLS1000 fluorometer. Different concentrations of A40-Cy3 were investigated for immobilization (200 nM, 500 nM, 1 µM, 2 µM) and the fluorescence signal from A40-Cy3 was acquired before and after immobilization of the aptamer on MBs; the amount of immobilized aptamer was assessed by difference. For the calculation, signals from the first two washing phases on modified-MBs were used to correct the signal of supernatant after immobilization.

Tables

Table S1. DNA and RNA sequences used in the present study. Variable regions are in bold, flanking regions are underlined.

Name	Sequence (5'-3')	Number of bases
A80	AGCAGCACAGAGGTCAGATG**GCAGCTAAGCAGGCGGCTCAC AAAACCATTCGCATGCGGC**CCTATGCGTGCTACCGTGAA	80
A40	**GCAGCTAAGCAGGCGGCTCACAAAACCATTCGCATGCGGC**	40
A80R	AGCAGCACAGAGGTCAGATG**ACTATGTCGGCCGCAATGCCC AGAGGCCACATACAAGCGG**CCTATGCGTGCTACCGTGAA	80
C80	GGGAATGGATCCACATCTACGAATTC**ATCAGGGCTAAAGAGT GCAGAGTTACTTAG**TTCACTGCAGACTTGACGAAGCTT	80
C30	**ATCAGGGCTAAAGAGTGCAGAGTTACTTAG**	30
C42	ATCTACGAATTC**ATCAGGGCTAAAGAGTGCAGAGTTACTTAG**	42
C80R	GGGAATGGATCCACATCTACGAATTC**AAGTGGATTAACTGTG TAGACCGATAGACG**TTCACTGCAGACTTGACGAAGCTT	80
PolyT40	TTTTTTTTTTTTTTTTTTTTTTTTTTTTTTTTTTTT	40
C80RNA	GGGAAUGGAUCCACAUCUACGAAUUC**AUCAGGGCUAAAGA GUGCAGAGUUACUUAG**UUCACUGCAGACUUGACGAAGCUU	80

Figures

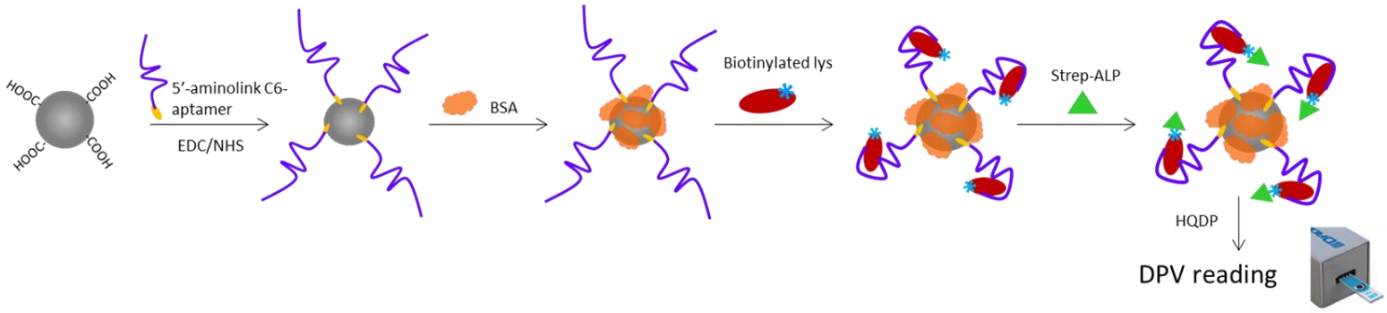

Figure S1. Scheme of the magneto-electrochemical apta-assay based on MBs.

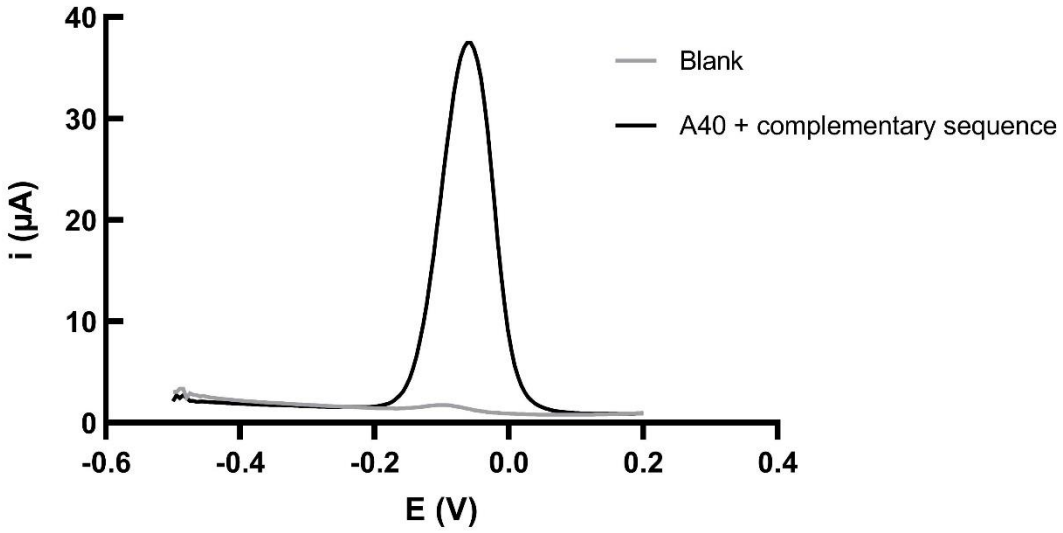

Figure S2. DPV voltammograms obtained with non-functionalized MBs (blank) and A40-modified MBs, in presence of the 20-mer sequence complementary to A40.

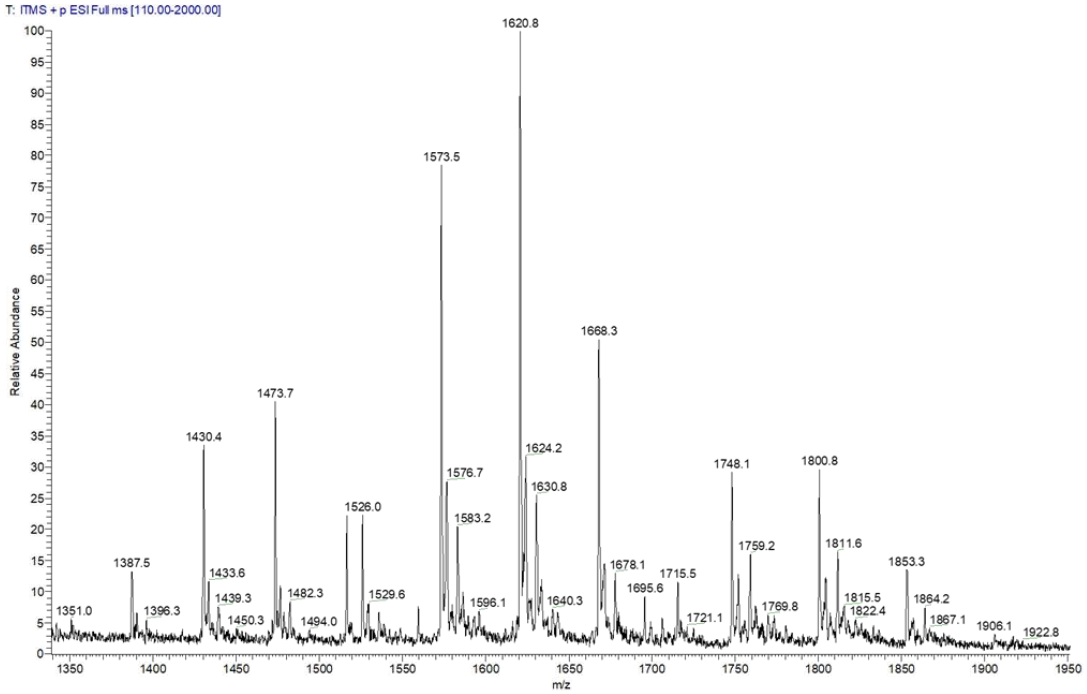

Figure S3. Full-scan ESI(+)-MS spectrum of biotinylated lysozyme.

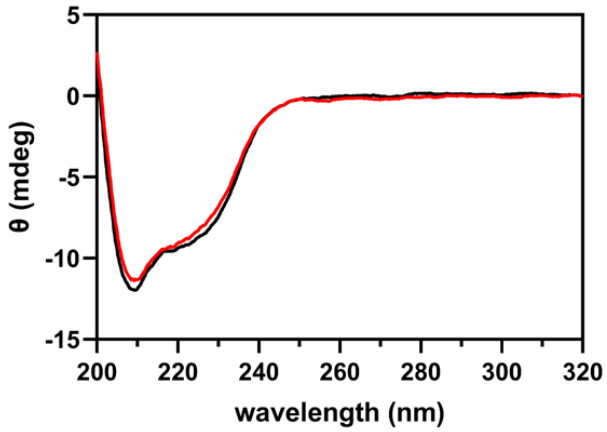

Figure S4. Overlay of CD spectra of unmodified (black) and biotinylated lysozyme (red).

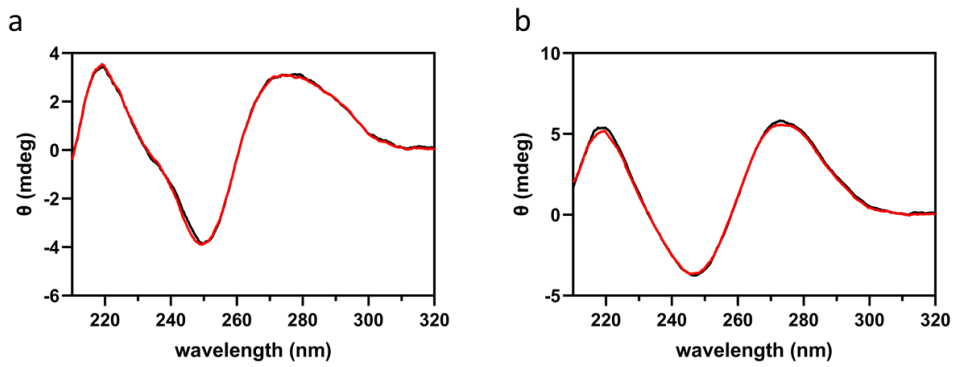

Figure S5. Overlay of CD spectra of (a) A40 and (b) C42 before and after denaturation/refolding experiments.

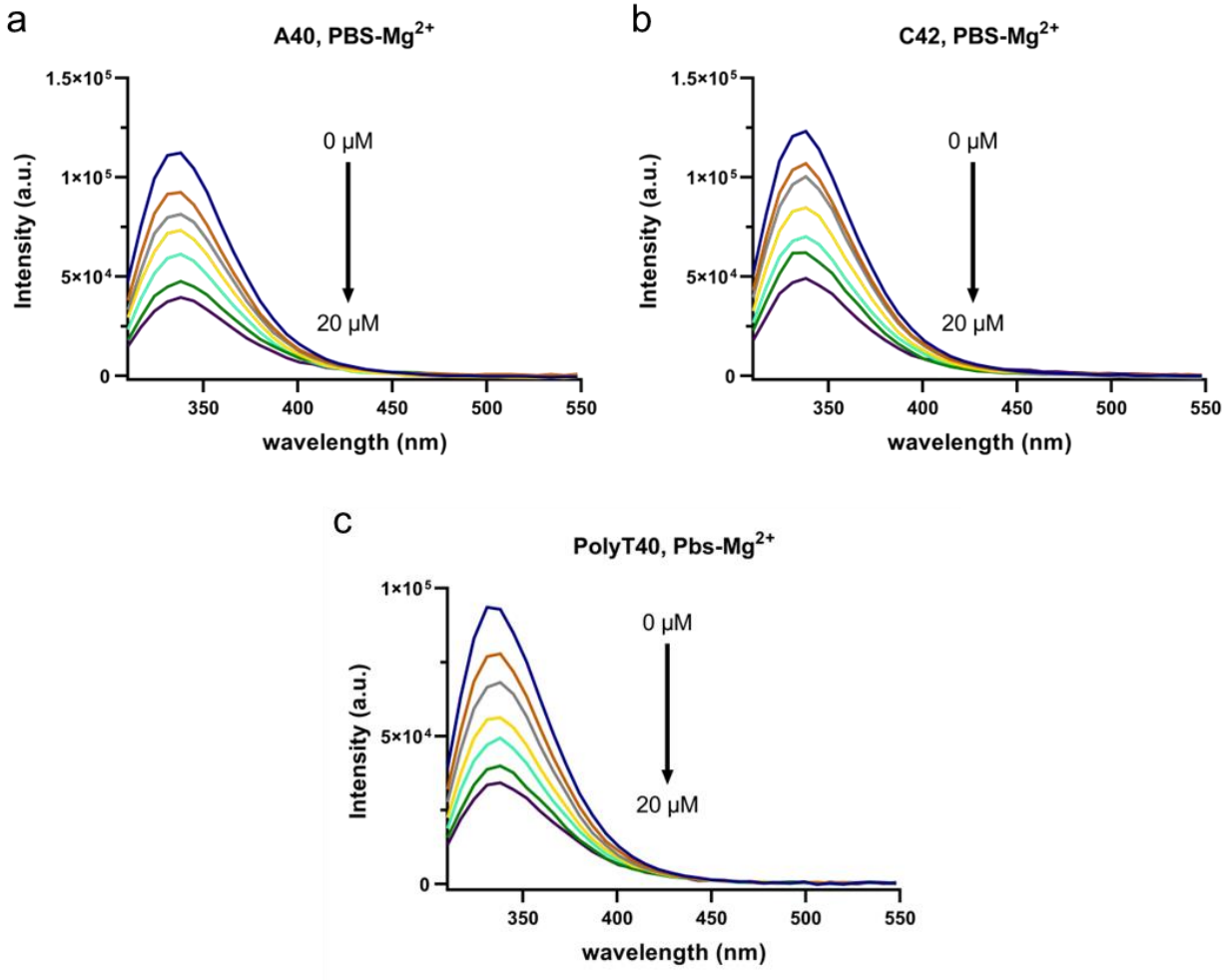

Figure S6. Fluorescence titration curves of lysozyme (1 μM solution, λexc = 298 nm) with (a) A40, (b) C42 and (c) PolyT40 sequences in PBS-Mg2+ buffer. The concentration of aptamer varied from 0 to 20 μM.

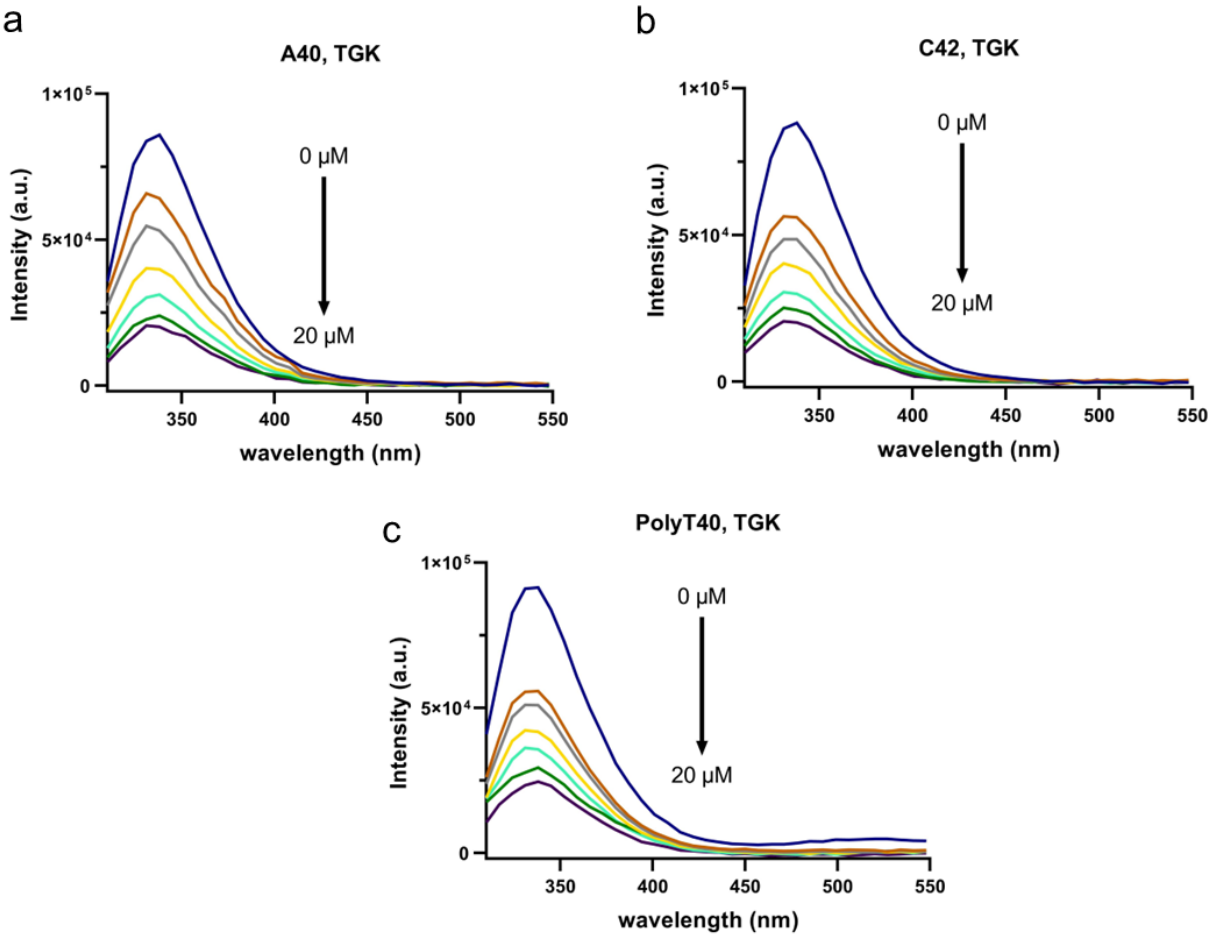

Figure S7. Fluorescence titration curves of lysozyme (1 μM solution, λ_{exc} = 298 nm) with (a) A40, (b) C42 and (c) PolyT40 sequences in TGK buffer. The concentration of aptamer varied from 0 to 20 μM.